

Vector Boson Fusion Topology and Simplified Models for Dark Matter Searches at Colliders

Santiago Duque-Escobar,^{*} Daniel Ocampo-Henao,[†] and José D. Ruiz-Álvarez[‡]
Instituto de Física, Universidad de Antioquia, A.A. 1226, Medellín, Colombia
(Dated: December 15, 2021)

In this paper, we study the possible searches at colliders using Vector Boson Fusion topology in the context of Simplified Models signatures. We examine the possible physics reach of these searches with regard to monojet-type searches, and determine how these two signatures are complementary. We determine the generic characteristics for dark matter signatures in the LHC if the underlying physics imply Vector Boson Fusion type of production.

I. INTRODUCTION

One of the most striking challenges in contemporary physics is to determine the nature of around a quarter of the matter content of the universe. This fraction is usually referred to as dark matter. We have several sources of evidence pointing to the existence of an unknown form of matter from different types of astronomical measurements [1, 2, 3, 4]. However, direct and indirect searches have failed to find a particle which could explain the dark matter abundance.

The quest towards dark matter discovery can be also pursued in particle colliders as the Large Hadron Collider (LHC). Several searches have been done by ATLAS and CMS experiments [5, 6, 7, 8, 9, 10], but still no positive indication of the production of a dark matter particle in the LHC has been found.

Several theoretical frameworks have been developed to explore dark matter searches at colliders. More specifically, the simplified models scheme [11, 12] constitute a useful benchmark modelling of dark matter production at the LHC that have been introduced in recent years. The simplified models provide a rather free theoretical approach and simple interpretation framework. Therefore, it is interesting to envisage all possible signatures for dark matter searches within the simplified model approach. It is very important to identify all the possibilities that can be pursued at the LHC within this modelling.

We study the possible Vector Boson Fusion (VBF) signatures that can be achieved within simplified models with dark matter production. We optimize the selections to enhance signal separation in VBF signatures with regard to standard model backgrounds. Our findings are then compared to monojet-type searches and show VBF signatures complementarity in dark matter searches.

In this paper we first discuss the simplified models and possible VBF signatures in section II, then we show the VBF cuts developed in section III. In section IV, we present our results and discuss them in regard of monojet-type searches, and we conclude in section V.

II. SIMPLIFIED MODELS FOR DARK MATTER SEARCHES AT THE LHC

Within the scope of performing searches for dark matter in colliders, many different approaches have been proposed. Possibly the first approach considered has been the neutralino candidate within a MSSM theoretical framework [13, 14]. However it has been quickly identified that such an approach is limited and present strong theoretical restrictions. Many more generic models have been proposed as the Inert Dark Matter model [15, 16]. These models too are limited for searches within the LHC as they are formerly constrained from a theory perspective.

Finally, the last step before the arrival of simplified models has been the effective field theory (EFT) approach [17, 18]. In this theory, the mediator that communicates the dark matter candidate with the SM is very heavy, and thus escaping the energy reach of the LHC. This has strong implications for the kinematic properties of the dark matter production signatures, making it extremely difficult to search for a dark matter candidate with a rather light mediator.

At this point, the simplified models were proposed as an intermediate solution among the EFT and complete models. The simplified models allow having a quite complete theoretical picture with a very unrestricted modelling and an easy framework for reinterpretations. Therefore, the simplified models can be used to inspire and design searches at the LHC, but can also be used to interpret LHC results and also export them into the context of complete models, as the MSSM.

The simplest formulation is a simplified model with a fermionic dark matter candidate and a scalar or vector mediator. The mediator couples only to quarks and dark matter. In the first case to allow the production of the additional mediator in the LHC from proton-proton collision. The second coupling ensures the decay of the mediator into dark matter particles. The main processes for dark matter production in a VBF topology for each of these models are shown in Fig. 1.

The two diagrams share a common structure, but for the scalar mediator case the two final hadronic particles are quarks while in the vector mediator case are gluons. Additionally, in the scalar mediator case the particles me-

^{*} asantiago.duque@udea.edu.co

[†] daniel.ocampoh@udea.edu.co

[‡] josed.ruiz@udea.edu.co

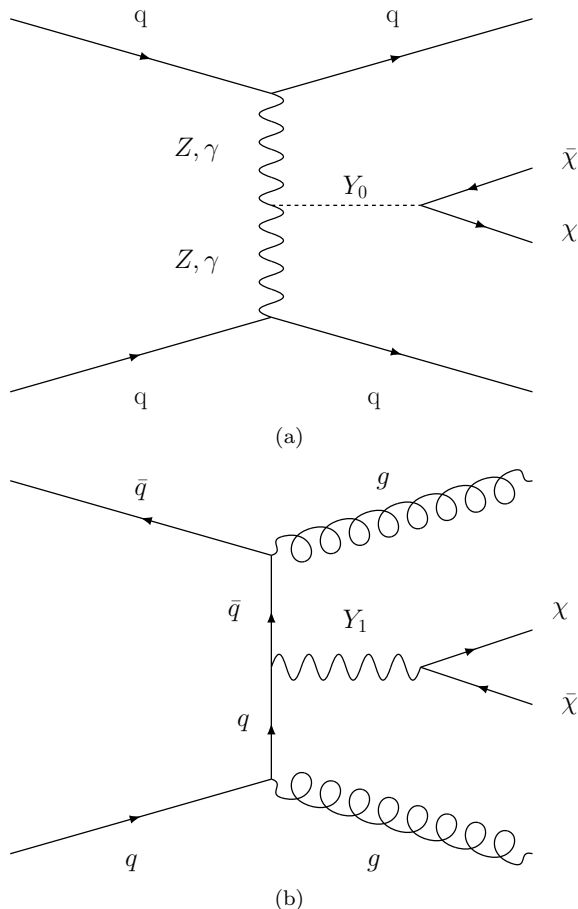


FIG. 1. Main processes for dark matter production in a VBF topology: a) Model with a scalar mediator. b) Model with a vector mediator.

diating the process are vector bosons from the SM and in the vector mediator case are quarks, which of course also implies a coupling of the new mediator to standard model bosons. Therefore, the scalar mediator case is an authentic VBF process, very similar to the VBF Higgs production mechanism. This fact allows us to explore the VBF production of dark matter in a Higgs-like mechanism, but with mediator masses that can be much greater. The vector mediator case is more exotic to dark matter searches, letting us explore new possible scenarios.

Moreover, the simplified models allow us to explore a very wide range of mediator masses as well as mediator couplings. These factors are key to our study and will be fully detailed in the next sections.

III. VECTOR BOSON FUSION SEARCHES

Since one of the main features of dark matter is its extremely small interaction with normal matter, all searches at colliders rely on the production of some visible particle recoiling against the dark matter, which will subsequently be tagged in the detector as missing trans-

verse momentum or energy p_T^{miss} . A common strategy to look for such events is the mono-jet search, already well studied in the context of collider searches [5]. It is also important to remark that the simplified models approach has born in the context of mono-jet searches.

VBF events are characterized by two interacting vector bosons and two deflected partons from the initial partons resulting in two forward jets plus p_T^{miss} . The main characteristics of the VBF topology that have been identified in the literature are a high invariant mass for the two VBF jets, a geometric location of these two jets in opposite hemispheres of the detector and a high η separation. This topology is an alternative and complementary strategy to look for dark matter at colliders. The VBF topology allows lower kinematic thresholds, resulting in non- p_T^{miss} based event selection [19]. The utility of the VBF topology has been shown in other beyond standard model contexts such as Higgs Portal dark matter and MSSM [6, 20].

A. Simulated event samples

The signal has been simulated from proton-proton collisions at $\sqrt{s} = 13$ TeV in a VBF topology with scalar or vectorial mediators. The signal samples were produced for several combinations of dark matter and mediator masses points (m_χ , m_Y), ranging from 10 to 1000 GeV and from 100 to 5000 GeV, respectively. The signal model used is a simplified dark matter model from FEYNRULES model database [12, 21, 22]. All the models were used in their UFO [23] implementation.

Electroweak bosons produced in association with jets are the primary backgrounds for this search, particularly, the production of a Z boson and jets, followed by the decay of the Z boson into neutrinos. In the present study we have simulated only Drell-Yan plus jets background and following [20] reasoning, we also consider that W +jets background kinematics are similar to Drell-Yan. Therefore, we assume the final background contribution composed 70% of Drell-Yan events and 30% of W +jets.

The partonic processes for signal and background events have been produced with MADGRAPH5_AMC (v2.8.2) [24]. The showering and hadronization have been performed by PYTHIA8 [25, 26], and the detector simulation has been done by DELPHES (v3.4.2) [27].

B. Event selection

We have developed an event selection optimizing the significance, defined as $\frac{S}{\sqrt{S+B}}$, using signal events both from scalar and vectorial mediators signals and from Drell-Yan background. We have noted that for both signals considered the optimization had the same results and therefore we end up with one selection regardless of the signal mediator type. The selection begins with very basic criteria mainly driven by well known detector require-

ments. This baseline selection is described in Table I. The total hadronic energy is defined as $H_T = \sum p_T(j)$ which is the scalar sum of the transverse momentum of all the jets in the event which have a $p_T > 30$ GeV. The criterion of $H_T > 200$ GeV is imposed in order to assure a minimum quantity of energy to assure signal events passing the detector trigger. This requirement prevents us to rely on missing transverse momentum for the trigger. We have seen that signal events don't have very high missing transverse momentum, and therefore the H_T criterion is very useful to avoid losing a large amount of signal events by the trigger.

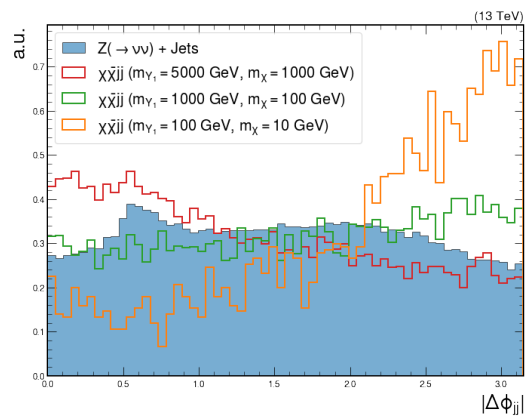
TABLE I. Baseline selection

Criterion	
Number of jets	> 1
$\eta(j_1) \cdot \eta(j_2)$	< 0
Leading jets p_T	> 30 GeV
Leading jets $ \eta $	< 5
H_T	> 200 GeV
p_T^{miss}	> 50 GeV

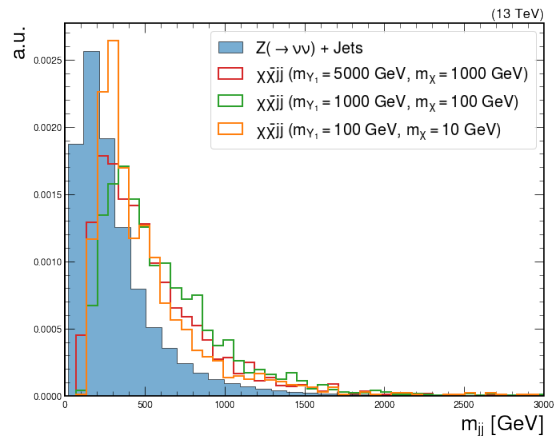
For events surviving the baseline selection, we have studied several variables that could potentially increase the signal over background separation. The most discriminant variables are found to be the azimuthal angle difference among the two leading jets $\Delta\phi_{jj}$, their invariant mass m_{jj} and their pseudorapidity separation $\Delta\eta_{jj}$. The first two variables have a homogeneous behavior for different mediator masses. However, it is not the same case for the pseudorapidity separation of the two leading jets. In consequence, we start our main selection based on criteria on the azimuthal difference of the leading jets and their invariant mass. Figure 2 show the distribution of signal and background events for $|\Delta\phi_{jj}|$ after baseline selection is applied and for m_{jj} after applying a selection also on the azimuthal angle separation.

From these two first requirements we apply a control criterion intended not for separation of signal with regard to electroweak backgrounds but to actually control the possible contribution from QCD processes to the background. The applied criterion is $\min|\Delta\phi(p_T^{miss}, j_i)| > 0.5$ for the first four leading jets, $i = \{1, 2, 3, 4\}$. This cut ensures having real missing transverse momentum and thus rejecting efficiently QCD events [6, 19].

Finally, we have noted that the variable $\Delta\eta_{jj}$ greatly depends on the mass of the mediator. For high mediator masses, above 1 TeV, $\Delta\eta_{jj}$ is restricted to low values, while for low mediator masses, below 1 TeV, the $\Delta\eta_{jj}$ is much higher. The most known scenario for VBF topology is for Higgs SM production, which corresponds to our low mass mediator case, from which a high $\Delta\eta_{jj}$ value has been identified as a characteristic feature of VBF, however we see that the pseudorapidity difference for the two VBF jets is not fixed and actually highly anti-correlated to the mediator mass. This finding is also supported by the work done in [28].



(a)



(b)

FIG. 2. Signals for vectorial mediator and background events distribution for [a] $|\Delta\phi_{jj}|$ variable on events passing the baseline selection, and [b] m_{jj} for events passing the baseline selection and $|\Delta\phi_{jj}| > 2.3$

In correspondence with this finding, we define two analysis bins optimized to keep events for the two mediator mass scenarios described. Table II summarizes the event selection and Figure 3 shows $|\Delta\eta_{jj}|$ for signal events and backgrounds after all other cuts.

TABLE II. Event selection. The last line specifies the two bin selections optimized for high and low mediator masses.

Feature	Value
$ \Delta\phi_{jj} $	> 2.3
m_{jj}	> 1000 GeV
$\min \Delta\phi(p_T^{miss}, j_i) $	> 0.5
$ \Delta\eta_{jj} $	< 2.5 or > 2.5

IV. RESULTS AND DISCUSSION

From the selection developed we establish its reach considering different dark matter and mediator masses.

The simplified models approach only depends on five parameters, the dark matter mass, the mediator mass, and the couplings of the mediator to quarks, to SM bosons and dark matter. We first establish the significance of the selection for fixed couplings for some benchmark masses. We then analyze the reach of the analysis for fixed masses while varying the couplings.

In Tables III, IV and V are shown the number of expected events, the significance and cut efficiency as the selection criteria are applied for the three benchmark masses for signal and background for 150 fb^{-1} . The expected number of events are calculated using the cross-sections obtained from MadGraph setting couplings of the mediator to dark matter $g_\chi = 1$, to standard model bosons $g_V = 1$ and to quarks $g_q = 0.25$. The cross-sections are shown for fixed mediator mass, fixed couplings and as a function of the dark matter mass in Figure 4.

Taking into account the dependence of the cross-sections to the couplings and to the mediator and dark matter mass, we have scanned the models parameters in order to identify the exclusion reach of the proposed selections. Figure 5 show the excluded areas in the quark coupling-mediator mass plane while having fixed dark matter mass and coupling fixed to 10 GeV and 1.0 respectively. It also shows the exclusion in the quark and

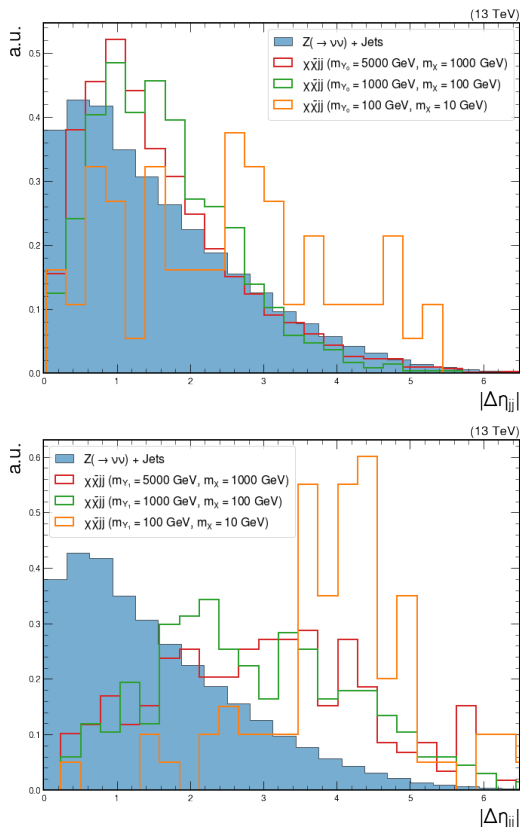


FIG. 3. Signals and background events distribution for $|\Delta\eta_{jj}|$ variable on events passing all the other criteria.

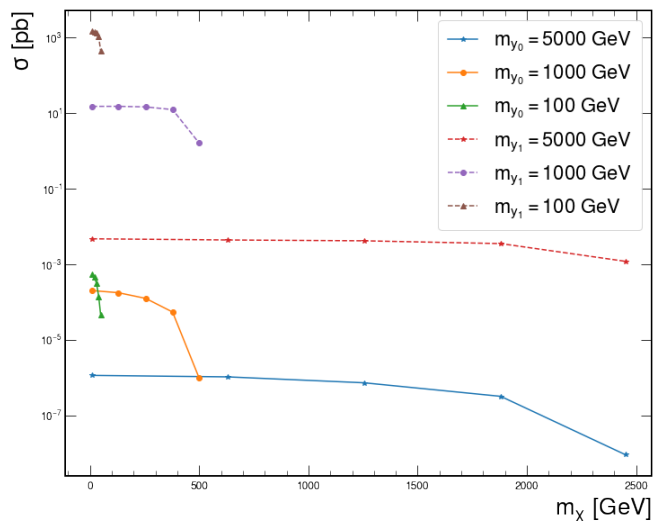


FIG. 4. Signals cross-sections for fixed mediator mass, as described in the legend, setting $g_\chi = 1$, $g_V = 1$ and $g_q = 0.25$ as a function of the dark matter candidate mass.

dark matter coupling of the mediator, with the mediator mass fixed to 1 TeV and dark matter mass fixed to 10 GeV. The excluded regions are built using a sensitivity of at least 5, and are depicted in the plots as a red line. We only reach exclusion for the vectorial mediator scenario.

V. CONCLUSIONS

From the results shown, we can state that VBF searches for dark matter show a reach up to 2 TeV in the mediator mass and down to 0.2 for the couplings in the vectorial mediator case. These results are compatible with the results achieved by monojet searches and complimentary because they impose limits on a different signature, which should be in nature if monojet process is allowed.

In addition, we could also cover the parameter space of the model in the mediator and dark matter mass plane up to values closer to the diagonal with the dark matter mass equal to half of the mediator mass than the ones already covered by monojet searches. But this would also imply an assumption over the width of the mediator in order to assure stable cross-sections and efficiencies up to the diagonal. In other words, the reach of VBF search is better in the mediator and dark matter mass plane for narrow width mediators (less than 10 GeV) with regard to monojet searches.

Finally, we have found that in order to have sensitive VBF searches we might need to optimize the selections depending on the mediator masses explored due to kinematic differences as the ones we have found for the difference in the pseudorapidity of the two VBF jets in the events.

TABLE III. Events after each selection applied for background and some signals, assuming a luminosity of 150fb^{-1} .

Selection	Scalar (m_{Y_0}, m_X) GeV			Vector (m_{Y_1}, m_X) GeV			B
	(100,10)	(1000,100)	(5000,1000)	(100,10)	(1000,100)	(5000,1000)	
Baseline	32.84	76.07	1.34	1.16e+7	4.67e+5	170.80	5.40e+8
$ \Delta\phi_{jj} $	29.19	66.76	1.33	5.89e+6	1.43e+5	37.47	1.49e+8
m_{jj}	14.23	52.05	1.33	5.07e+5	1.89e+4	4.65	2.17e+7
$\min \Delta\phi(p_T^{miss}, j_i) $	1.56	10.02	0.26	3.00e+5	1.02e+4	2.65	1.43e+7
$ \Delta\eta_{jj} $	0.72, 0.84	8.30, 1.72	0.22, 0.04	2.43e+4, 2.76e+5	4.54e+3, 5.70e+3	1.07, 1.57	2.77e+6, 1.15e+7

TABLE IV. Significance defined as $\frac{S}{\sqrt{S+B}}$ for each signal and including the scale factor for background to include W+jets contribution, assuming a luminosity of 150fb^{-1} .

Selection	Scalar (m_{Y_0}, m_X) GeV			Vector (m_{Y_1}, m_X) GeV		
	(100,10)	(1000,100)	(5000,1000)	(100,10)	(1000,100)	(5000,1000)
Baseline	1.24e-3	2.87e-3	5.08e-5	4.37e+2	1.76e+1	6.44e-3
$ \Delta\phi_{jj} $	2.10e-3	4.80e-3	9.59e-5	4.18e+2	1.03e+1	2.69e-3
m_{jj}	2.68e-3	9.78e-3	2.51e-4	9.46e+1	3.56	8.76e-4
$\min \Delta\phi(p_T^{miss}, j_i) $	3.62e-4	2.32e-3	6.12e-5	6.91e+1	22.37	6.14e-4
$ \Delta\eta_{jj} $	3.82e-4, 2.16e-4	4.38e-3, 4.45e-4	1.16e-4, 1.15e-5	1.28e+1, 7.06e+1	2.39, 1.47	5.65e-4, 4.07e-4

ACKNOWLEDGMENTS

The authors gratefully acknowledge the support of the Colombian Science Ministry MinCiencias and Sostenibilidad-UdeA. J.D.R.A also acknowledge the welcoming of the Instituto de Física Corpuscular (IFIC) from Valencia, Spain, during the completion of this work.]

-
- [1] K. Griest, The Search for dark matter: WIMPs and MACHOs, *Annals N. Y. Acad. Sci.* **688**, 390 (1993), arXiv:hep-ph/9303253.
- [2] V. C. Rubin, The rotation of spiral galaxies, *Science* **220**, 1339 (1983).
- [3] R. Minchin, J. Davies, M. Disney, P. Boyce, D. Garcia, C. Jordan, V. Kilborn, R. Lang, S. Roberts, S. Sabatini, *et al.*, A dark hydrogen cloud in the virgo cluster, *The Astrophysical Journal Letters* **622**, L21 (2005).
- [4] V. Zacek, Dark Matter, in *22nd Lake Louise Winter Institute: Fundamental Interactions* (2007) pp. 170–206, arXiv:0707.0472 [astro-ph].
- [5] A. M. Sirunyan *et al.* (CMS), Search for new physics in final states with an energetic jet or a hadronically decaying W or Z boson and transverse momentum imbalance at $\sqrt{s} = 13$ TeV, *Phys. Rev. D* **97**, 092005 (2018), arXiv:1712.02345 [hep-ex].
- [6] A. M. Sirunyan *et al.* (CMS), Search for supersymmetry with a compressed mass spectrum in the vector boson fusion topology with 1-lepton and 0-lepton final states in proton-proton collisions at $\sqrt{s} = 13$ TeV, *JHEP* **08**, 150, arXiv:1905.13059 [hep-ex].
- [7] A. M. Sirunyan *et al.* (CMS), Search for dark matter particles produced in association with a Higgs boson in proton-proton collisions at $\sqrt{s} = 13$ TeV, *JHEP* **03**, 025, arXiv:1908.01713 [hep-ex].
- [8] G. Aad *et al.* (ATLAS), Search for new phenomena in events with an energetic jet and missing transverse momentum in pp collisions at $\sqrt{s} = 13$ TeV with the ATLAS detector, *Phys. Rev. D* **103**, 112006 (2021), arXiv:2102.10874 [hep-ex].
- [9] G. Aad *et al.* (ATLAS), Search for dark matter produced in association with a single top quark in $\sqrt{s} = 13$ TeV pp collisions with the ATLAS detector, *Eur. Phys. J. C* **81**, 860 (2021), arXiv:2011.09308 [hep-ex].
- [10] A. M. Sirunyan *et al.* (CMS), Search for dark matter produced in association with a leptonically decaying Z boson in proton-proton collisions at $\sqrt{s} = 13$ TeV, *Eur. Phys. J. C* **81**, 13 (2021), [Erratum: *Eur.Phys.J.C* **81**, 333 (2021)], arXiv:2008.04735 [hep-ex].
- [11] J. Abdallah, A. Ashkenazi, A. Boveia, G. Busoni, A. De Simone, C. Doglioni, A. Efrati, E. Etzion, J. Gramling, T. Jacques, *et al.*, Simplified models for dark matter and missing energy searches at the LHC, arXiv preprint arXiv:1409.2893 (2014).
- [12] J. Abdallah *et al.*, Simplified Models for Dark Matter Searches at the LHC, *Phys. Dark Univ.* **9-10**, 8 (2015), arXiv:1506.03116 [hep-ph].
- [13] C. Csaki, The Minimal supersymmetric standard model (MSSM), *Mod. Phys. Lett. A* **11**, 599 (1996), arXiv:hep-ph/9606414.
- [14] H. E. Haber, The Status of the minimal supersymmetric

TABLE V. Criteria efficiency for each signal point considered and for background.

Selection	Scalar (m_{Y_0}, m_X) GeV			Vector (m_{Y_1}, m_X) GeV			B
	(100,10)	(1000,100)	(5000,1000)	(100,10)	(1000,100)	(5000,1000)	
Baseline	0.041	0.203	0.659	0.071	0.226	0.271	0.293
$ \Delta\phi_{jj} $	0.889	0.878	0.991	0.505	0.308	0.219	0.276
m_{jj}	0.488	0.780	1.000	0.086	0.132	0.124	0.146
$\min \Delta\phi(p_T^{miss}, j_i) $	0.110	0.193	0.198	0.592	0.541	0.569	0.659
$ \Delta\eta_{jj} $	0.464, 0.536	0.828, 0.172	0.832, 0.168	0.081, 0.919	0.444, 0.556	0.405, 0.595	0.193, 0.807

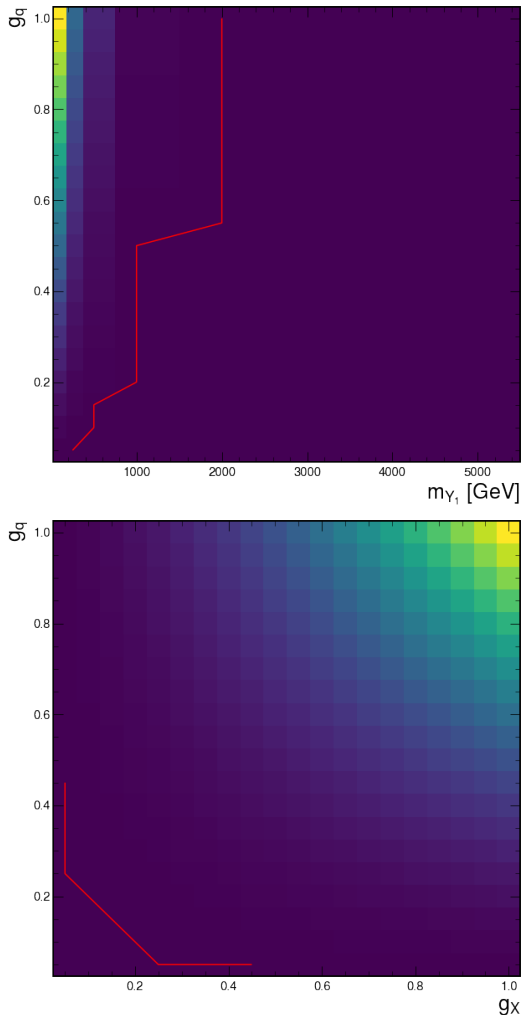


FIG. 5. Exclusion reach of the selections for [left] g_q -mediator mass where the excluded region is from the red line for greater couplings and smaller mediator masses, and for [right] g_q - g_X plane with the excluded region from the red line towards higher couplings.

standard model and beyond, Nucl. Phys. B Proc. Suppl. **62**, 469 (1998), arXiv:hep-ph/9709450.

- [15] E. M. Dolle and S. Su, The Inert Dark Matter, Phys. Rev. D **80**, 055012 (2009), arXiv:0906.1609 [hep-ph].

- [16] A. Goudelis, B. Herrmann, and O. Stål, Dark matter in the Inert Doublet Model after the discovery of a Higgs-like boson at the LHC, JHEP **09**, 106, arXiv:1303.3010 [hep-ph].
- [17] H. Georgi, Effective field theory, Annual review of nuclear and particle science **43**, 209 (1993).
- [18] C. P. Burgess, Introduction to Effective Field Theory, Ann. Rev. Nucl. Part. Sci. **57**, 329 (2007), arXiv:hep-th/0701053.
- [19] A. M. Sirunyan *et al.* (CMS), Search for invisible decays of a Higgs boson produced through vector boson fusion in proton-proton collisions at $\sqrt{s} = 13$ TeV, Phys. Lett. B **793**, 520 (2019), arXiv:1809.05937 [hep-ex].
- [20] B. Dutta, G. Palacio, J. D. Ruiz-Alvarez, and D. Restrepo, Vector Boson Fusion in the Inert Doublet Model, Phys. Rev. D **97**, 055045 (2018), arXiv:1709.09796 [hep-ph].
- [21] J. Abdallah *et al.*, Simplified Models for Dark Matter and Missing Energy Searches at the LHC, (2014), arXiv:1409.2893 [hep-ph].
- [22] M. R. Buckley, D. Feld, and D. Goncalves, Scalar Simplified Models for Dark Matter, Phys. Rev. D **91**, 015017 (2015), arXiv:1410.6497 [hep-ph].
- [23] C. Degrande, C. Duhr, B. Fuks, D. Grellscheid, O. Mattelaer, and T. Reiter, UFO - The Universal FeynRules Output, Comput. Phys. Commun. **183**, 1201 (2012), arXiv:1108.2040 [hep-ph].
- [24] J. Alwall, R. Frederix, S. Frixione, V. Hirschi, F. Maltoni, O. Mattelaer, H. S. Shao, T. Stelzer, P. Torrielli, and M. Zaro, The automated computation of tree-level and next-to-leading order differential cross sections, and their matching to parton shower simulations, JHEP **07**, 079, arXiv:1405.0301 [hep-ph].
- [25] T. Sjöstrand, S. Mrenna, and P. Z. Skands, PYTHIA 6.4 Physics and Manual, JHEP **05**, 026, arXiv:hep-ph/0603175.
- [26] T. Sjöstrand, S. Ask, J. R. Christiansen, R. Corke, N. Desai, P. Ilten, S. Mrenna, S. Prestel, C. O. Rasmussen, and P. Z. Skands, An introduction to PYTHIA 8.2, Comput. Phys. Commun. **191**, 159 (2015), arXiv:1410.3012 [hep-ph].
- [27] J. de Favereau, C. Delaere, P. Demin, A. Giammanco, V. Lemaitre, A. Mertens, and M. Selvaggi (DELPHES 3), DELPHES 3, A modular framework for fast simulation of a generic collider experiment, JHEP **02**, 057, arXiv:1307.6346 [hep-ex].
- [28] A. Flórez, A. Gurrola, W. Johns, J. Maruri, P. Sheldon, K. Sinha, and S. R. Starko, Anapole Dark Matter via Vector Boson Fusion Processes at the LHC, Phys. Rev. D **100**, 016017 (2019), arXiv:1902.01488 [hep-ph].